Modulation of Mid-Atlantic Tropical Cyclone Landfalls by the MJO

Julia V. Manganello, and James L. Kinter III

Center for Ocean-Land-Atmosphere Studies, George Mason University, Fairfax, Virginia

Corresponding author: Julia V. Manganello (jvisneva@gmu.edu) and James L. Kinter (ikinter@gmu.edu))

Key Points:

- A high-atmospheric-resolution seasonal prediction system is used to investigate the link between mid-Atlantic TC landfalls and the MJO
- Significant peak TC landfall frequencies over the U.S. mid-Atlantic region occur during MJO phases 1-3
- In the extended range (between 6- to 12-day lead times), MJO phases 1 and 2 are strongly favored

Abstract

In this study, we investigate the relationship between mid-Atlantic tropical cyclone (TC) landfalls and the Madden-Julian oscillation (MJO). This is done by using a high-atmoshperic-resolution ensemble prediction system based on the ECMWF operational model (Project Minerva) to compile the statistics of these rare events, and the velocity potential MJO (VPM) index to define the phase and amplitude of the MJO. We find that these TC landfalls are most likely to occur during VPM phases 1-3. At shorter lead times, phase 1 is strongly favored, with some contribution of phase 3. At longer lead times (between the 6- and 12-day leads), phases 1 and 2 consistently show significant TC landfall frequencies. This result suggests a potential for extended-range predictions of the mid-Atlantic TC landfall risk based on the phase of the MJO.

Plain Language Summary

Tropical cyclone (TC) landfalls over the U.S. mid-Atlantic region are very infrequent. However, when they do occur, the resulting human and material losses can be severe, as was recently the case with Hurricane Sandy in 2012. Therefore, it is important to be able to predict these land-falling events as far in advance as possible. In this study, we investigate the relationship between mid-Atlantic TC landfalls and the Madden-Julian oscillation (MJO), which is the dominant source of climate variability in the tropics on intraseasonal time scales (within a season). To do so, we use numerical simulations conducted with a high-atmoshperic-resolution ensemble prediction system based on the ECMWF operational model to compile the statistics of these rare events. The phase and magnitude of the MJO is determined using the velocity potential MJO (VPM) index. We find that mid-Atlantic TC landfalls are most likely to occur during VPM phases 1-3. At shorter lead times, phase 1 is strongly favored, with some contribution of phase 3. At longer lead times (between the 6- and 12-day leads), phases 1 and 2 are consistently preferred. This result suggests a potential for extended-range predictions of the mid-Atlantic TC landfall risk based on the phase of the MJO.

1 Introduction

Tropical cyclones (TCs) are one of the most hazardous extreme weather events that can lead to large human and material losses when they come in close proximity to land. Although being considered as one of the most infrequent landfalls along the U.S. East Coast, TC landfalls over the mid-Atlantic[1], when they do occur, can have devastating consequences due to large concentration of population and wealth in the region. A recent example is Hurricane Sandy in 2012 (Blake et al., 2013; NHC, 2018).

TC landfall is a complex phenomenon as its probability depends on the following fundamental factors: 1) genesis, 2) development (the intensity life cycle), and 3) the shape of track (the storm's ability to approach the coastline; Dailey et al., 2009). The Madden-Julian oscillation (MJO), which is the leading intraseasonal mode of atmospheric and oceanic variability in the tropics (see Li (2014) for a review), is found to influence some of these aspects of the North Atlantic TC activity. The MJO is a global-scale oscillation in circulation coupled to large-scale variations in convection. Its characteristic feature is the eastward propagation from

[1] Specified here as the coastlines of Virginia, Chesapeake Bay, Delmarva Peninsula, and New Jersey.

the Indian Ocean into the central Pacific where the upper tropospheric anomalies of zonal wind and the velocity potential are observed to circle the globe in about 50 days (Madden and Julian, 1994). This periodicity represents a major source of predictability on subseasonal time scales. Associated with the MJO variability are large-scale variations in upper- and lower-level winds, temperature, sea level pressure, convection, atmospheric moisture content, and sea surface temperature. Through these changes and related variations in vertical wind shear (VWS), low-level vorticity and the African easterly wave (AEW) activity, the MJO has been found to modulate TC genesis and development in the North Atlantic (Mo, 2000; Barrett and Leslie, 2009; Vitart, 2009; Klotzbach, 2010; Ventrice et al., 2011; Klotzbach and Oliver, 2015), the overall North Atlantic TC landfall activity (Barrett and Leslie, 2009; Vitart, 2009) and the U.S. TC landfall frequency (Klotzbatch, 2010). The increase of TC activity has been found to occur during the phases of the MJO corresponding to the enhanced convection over parts of Africa and the Indian Ocean and suppressed convection over the tropical Pacific. However, any effects of the MJO on the likelihood of storm recurvature by means of, e.g., changes in the mid-latitude flow patterns have not been identified in the studies above.

The role of the MJO in the genesis, life cycle and track changes of Hurricane Sandy has also been investigated. Shen et al. (2013) and Xiang et al. (2015) have both found the genesis of Hurricane Sandy to be highly predictable with a maximum prediction lead time of up to 6 and 11 days, respectively. This relatively high predictability of formation, initial development and propagation was partly attributed to the role of the MJO and its skillful prediction. Xiang et al. (2015) have also predicted Sandy's landfall location and time with one-week lead time (after the genesis has occurred). The authors hypothesized that the predictability source for the landfall of Sandy may also be linked to the MJO. A recent study of Ding et al. (2019) has specifically addressed predictability of Sandy's steering flow. They found that this flow was primarily controlled by a pair of anticyclonic and cyclonic intraseasonal-scale circulation systems. The anticyclone to the north was part of a global wave train triggered by the MJO heating in the tropical Indian Ocean. Accurate simulation of this meridional dipole structure was shown to be a key for a successful extended-range prediction of Sandy's track.

Using a high-atmospheric-resolution coupled prediction system, Manganello et al. (2019) have assessed predictability of all mid-Atlantic TC landfalls that in addition to the so-called Sandy-like, or westward-curving, tracks also include the late recurving systems like Hurricanes Bertha (1996) and Floyd (1999). Results of this study echo some of the findings of Ding et al. (2019). For example, mean atmospheric circulation anomalies during these land-falling events were found to be similar to the large –scale flow patterns that occurred during Hurricane Sandy. Their analysis using local finite-amplitude wave activity diagnostic (LWA; Huang and Nakamura, 2016) revealed large-amplitude quasi-stationary features extending from the North Atlantic to the North Pacific that persist up to about a week leading to these TC landfalls. In addition, the concurrent atmospheric flow changes over the tropical Atlantic, which were found to be favorable for TC formation and development, were accompanied by coherent anomalies in the tropical Indian Ocean indicative of the enhanced convection in the region.

Motivated by the studies above, we extend the analysis of Manganello et al. (2019) here to investigate a potential link between mid-Atlantic TC landfalls and the MJO. For this purpose, we use (1) ensemble seasonal hindcasts to simulate these rare land-falling events and (2) the velocity potential MJO (VPM) index of Ventrice et al. (2013) as an MJO phase and amplitude diagnostic. We demonstrate that the MJO significantly modulates mid-Atlantic TC landfalls in this set of simulations suggesting a possibility of extended-range dynamical TC landfall risk predictions in the region beyond the short-range predictions as shown in Manganello et al. (2019). Model and observational data and numerical methods are briefly introduced in section 2. Results are presented in section 3. Discussion and some concluding remarks are provided in section 4.

2 Data and Methodology

2.1 Model and observational data

In lieu of the very few occurrences of mid-Atlantic TC landfalls in the observational record (see Manganello et al., 2019), we use here ensemble seasonal hindcasts performed with the Minerva forecasting system to compile the statistics of these rare events. It is an experimental coupled prediction system (EPS) based on the European Centre for Medium-Range Weather Forecasts (ECMWF) System 4 (see Manganello et al. (2016) for full details). The Nucleus for European Modeling of the Ocean (NEMO; Madec, 2008) version 3.0 is the ocean component model of this EPS. It has the ORCA1 grid with a horizontal resolution of about 1° (and the equatorial refinement of 1/3°) and 42 levels in the vertical. The atmospheric component model is the ECMWF Integrated Forecasting System (IFS; European Centre for Medium-Range Weather Forecasts, 2013), cycle 38r1, which is a spectral, semi-implicit, semi-Lagrangian hydrostatic model with 91 levels in the vertical, and a model top in the mesosphere at 0.01 hPa. The unperturbed initial conditions for the atmosphere come from the ECMWF interim reanalysis (ERA-I; Dee et al., 2011) and Ocean ReAnalysis System 4 (ORA-S4) for the ocean.

In this study, we use experiments where the IFS is integrated at spectral T1279 horizontal resolution (referred to as T1279 hereafter), corresponding approximately to 16-km grid spacing. Minerva retrospective forecasts are initialized on May 1 during 1980-2013, are of 7-month duration and consist of 15 ensemble members, which effectively represents 510 May-November (MJJASON) seasons. Upper-air data truncated at spectral T42 resolution are available for the analysis. For the observational estimates of upper-air fields, we use the ERA-I at 0.703° x ~0.702° horizontal resolution for the same MJJASON season of 1980-2013. The ERA-I data were downloaded form the Research Data Archive at the National Center for Atmospheric Research, Computational and Information Systems Laboratory (https://doi.org/10.5065/D6CR5RD9, accessed 24 July 2019).

2.2 Numerical Methods

2.2.1 Identification and tracking of tropical cyclones

Simulated TCs are identified explicitly in the model data based on the tracking algorithm of Hodges (1994, 1995, 1999). Vortices are detected as maxima in the 6-hourly relative vorticity field averaged between 850- and 600-hPa levels with a threshold value of 5×10^{-6} s^{-1} (at a spectral resolution of T63). To separate TCs from the raw tracks, a post-tracking lifetime filter of 2 days and a set of TC identification criteria are applied. The latter include an 1) intensity (10-m wind speed) threshold equivalent to the observed tropical storm intensity, 2) warm core condition, 3) coherent vertical structure condition, 4) duration requirement where the criteria 1-3 need to be jointly attained for at least 24 hours at some point during the life cycle of a storm, and 5) geographic extent of the first identification (0°-20°N over land and 0°-30°N over oceans).

A mid-Atlantic TC landfall is considered to take place when: 1) the mid-Atlantic coastline is intersected from the sea by a TC track; or 2) the water-to-land transition occurring along the Chesapeake Bay or Delmarva coastlines is preceded by landfall in North Carolina. Although we do not consider only primary landfalls, if a TC makes landfall as described above more than once only the first occurrence is counted. Further details on TC identification and landfall definition in the mid-Atlantic are provided in Manganello et al. (2019).

2.2.2 MJO diagnosis

The daily state (phase and magnitude) of the MJO is determined using the velocity potential MJO (VPM) index of Ventrice et al. (2013). It consists of the leading pair of principal components (PCs) from a combined empirical orthogonal function (EOF) analysis of meridionally averaged (15°N-15°S) 200-hPa zonal wind (U200), 850-hPa zonal wind (U850) and 200-hPa velocity potential (VP200). This index is therefore similar in construction to the Real-time Multivariate MJO (RMM) index of Wheeler and Hendon (2004) except it uses VP200 instead of the outgoing longwave radiation. This change results in better discrimination of the MJO signal during boreal summer using the VPM index compared to the RMM index, including somewhat stronger and more coherent modulation of Atlantic TC activity (Ventrice et al., 2013).

The VPM index is applied to ERA-I data following the methodology outlined in Ventrice et al. (2013) except that the data are additionally downgraded to T42 for the direct comparison and use with hindcasts (see Text S1 for details). To diagnose the MJO in the simulations, we first perform a combined EOF analysis of the ensemble mean retrospective forecast anomalies of U200, U850 and VP200. These input fields are initially processed following in part the methodology described in Gottschalck et al. (2010) and Vitart (2017). The obtained eigenvectors (spatial structures of the leading two EOFs), which realistically capture the observed meridional structure of the MJO (compare Figs. S1 and S2), form the basis of the VPM index calculation for every ensemble member of the hindcasts. This is done by projecting daily anomalies from each individual ensemble member on these model eigenvectors and normalizing resultant time series to produce the two-component VPM index (a detailed description of this procedure is provided in Text S2).

3 Results

The composite evolution of the MJO during the extended summer season of May to October, as characterized here by atmospheric large-scale upper-level divergence and low-level winds, is shown in Fig. 1. Similar to the RMM index, the phase information of the VPM index allows classification of the MJO into eight phases corresponding to a time when it is located over a specific geographical region. The MJO starts with enhanced convection over the Indian Ocean where it increases in geographical extent and amplitude and moves northward and eastward (phases 1-3; see Figs. 1a-c). It then propagates across the Maritime continent and into the Pacific (phases 4-6; Figs. 1d-f) where a simultaneous northward and eastward propagation is particularly evident in phase 4. The MJO then continues its transit across the Western Hemisphere during phases 7-8 (Figs. 1g-h). In the Atlantic sector, there are indications of enhanced upper-atmospheric divergence/convection during phases 7-8 and 1 and anomalous lower-tropospheric westerlies over the tropical North Atlantic during phases 1-3. Convective signal over tropical Africa is observed during phases 8, 1-2 including near-equatorial westerly anomalies over the western part of the continent during phases 2 and 3.

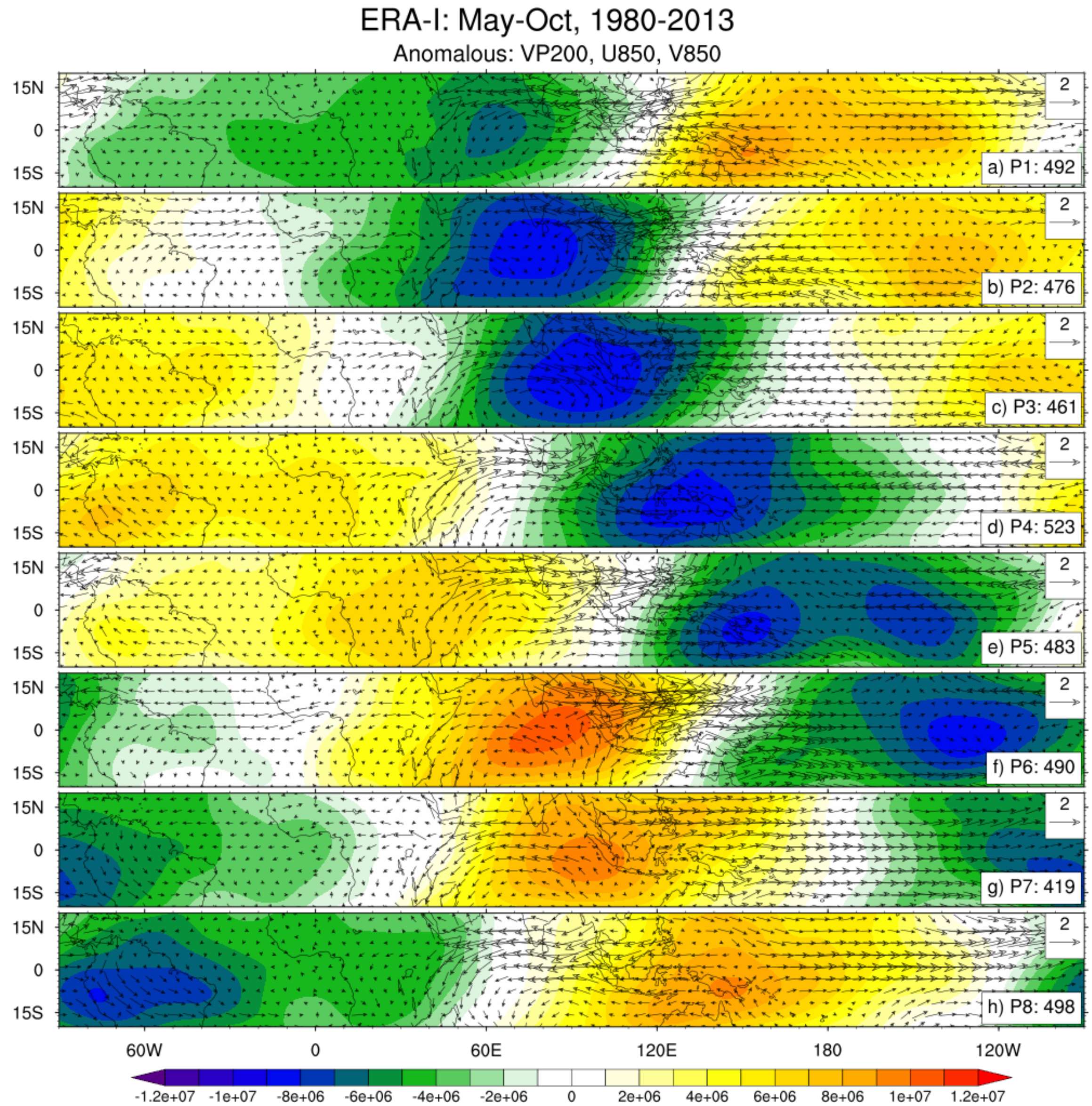

Figure 1: ERA-I MJJASO (1980-2013) composites of anomalous VP200 (shaded) and 850-hPa wind anomalies (vectors) for each MJO phase (indicated in the caption of each panel after letter "P") using the VPM index. Composites are made by averaging over the set of all days for a particular phase when amplitudes of the index are greater than one standard deviation. Total number of days is listed in the caption of each panel. Negative VP200 anomalies represent upper-level divergence. Units are m^2s^{-1}. The reference vector is 2 ms^{-1}.

Minerva T1279 hindcasts broadly capture the overall phasing and eastward propagation of the MJO, as shown by the ensemble-mean composite anomalies in Fig. 2., where a number of deficiencies are also noted. Apart from mostly weaker magnitudes, upper-level divergence during phases 1-4 (Figs. 2a-d) shows a systematic westward shift, slower propagation across the Indian Ocean and no apparent indication of the northward and eastward propagation split compared to observations. While the eastward propagation in the Pacific is also slower during phases 5-8 (Figs. 2e-h), there is, in addition, a relative reduction in the amplitude of the MJO in the eastern Pacific and over South America in phases 7 and 8. These amplitude and phase speed errors are common among ensemble forecasting systems with the ECMWF model generally displaying smaller errors (Vitart, 2017). Results in Fig. 2 suggest that convection over the Indian Ocean takes place mostly during phases 2 and 3, and over Africa during phases 1-3. Upper-level divergence over the tropical North Atlantic is present during phases 8 and 1-2. However, the occurrence of anomalous low-level westerlies over the tropical North Atlantic shows correct phasing (1-3).

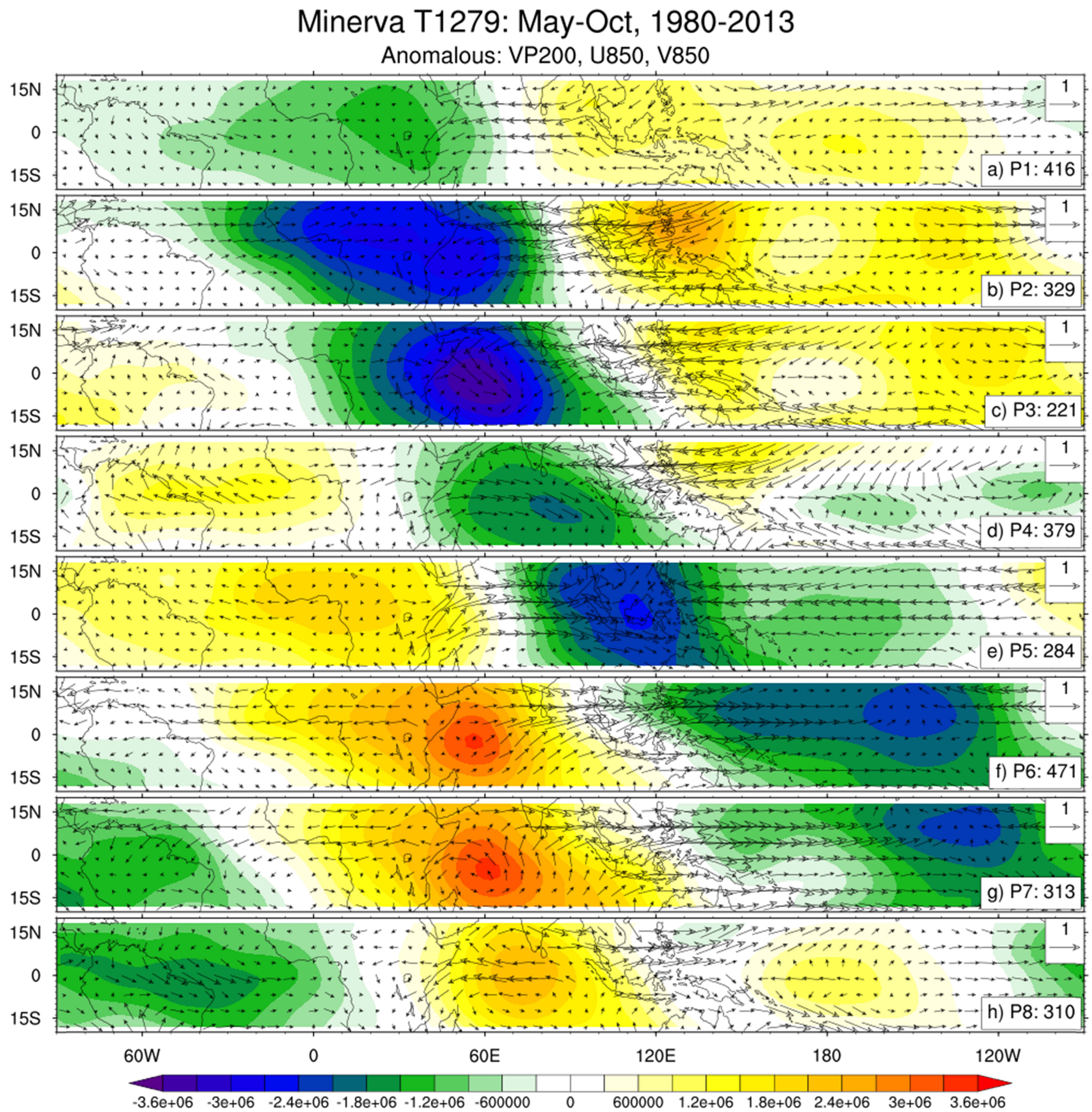

Figure 2: The same as in Fig. 1 but for the ensemble-mean T1279 hindcast data. The reference vector is 1 m/s.

To investigate whether mid-Atlantic TC landfalls vary coherently with the MJO phase as represented by the model VPM PCs, the land-falling events at leads ranging from 14 days to the landfall are binned by each phase of the MJO when the corresponding MJO amplitude is greater or equal to one (standard deviation). The resulting frequencies are displayed in Fig. 3. Confidence intervals are obtained by selecting randomly with replacement from all July-October anomalies (the seasonal extent of these TC landfalls) a total number of days that the MJO is greater than one for each MJO index phase. This procedure is done 50,000 times and the results are sorted. The computed 10% and 90% confidence intervals are displayed by box plots in Fig. 3. We find that mid-Atlantic TC landfalls occur more often during VPM phases 8 and 1-3 compared to phases 4-7. Statistically significant peak landfall frequencies are obtained during VPM phases 1-3 at multiple lead times. Phase 6 is the least likely to be associated with the land-falling events as the landfall frequencies during this phase are largely below the 10^{th} percentile (Fig. 3b). Our results also suggest that at longer lead times (between 6- and 12-day leads), phases 1 and 2 are strongly favored (Fig. 3a). At shorter leads, it is predominantly phase 1 and possibly phase 3. When the MJO amplitude is not considered, the results are qualitatively similar except that the TC landfall frequencies are relatively lower in phases 1-3 (not shown).

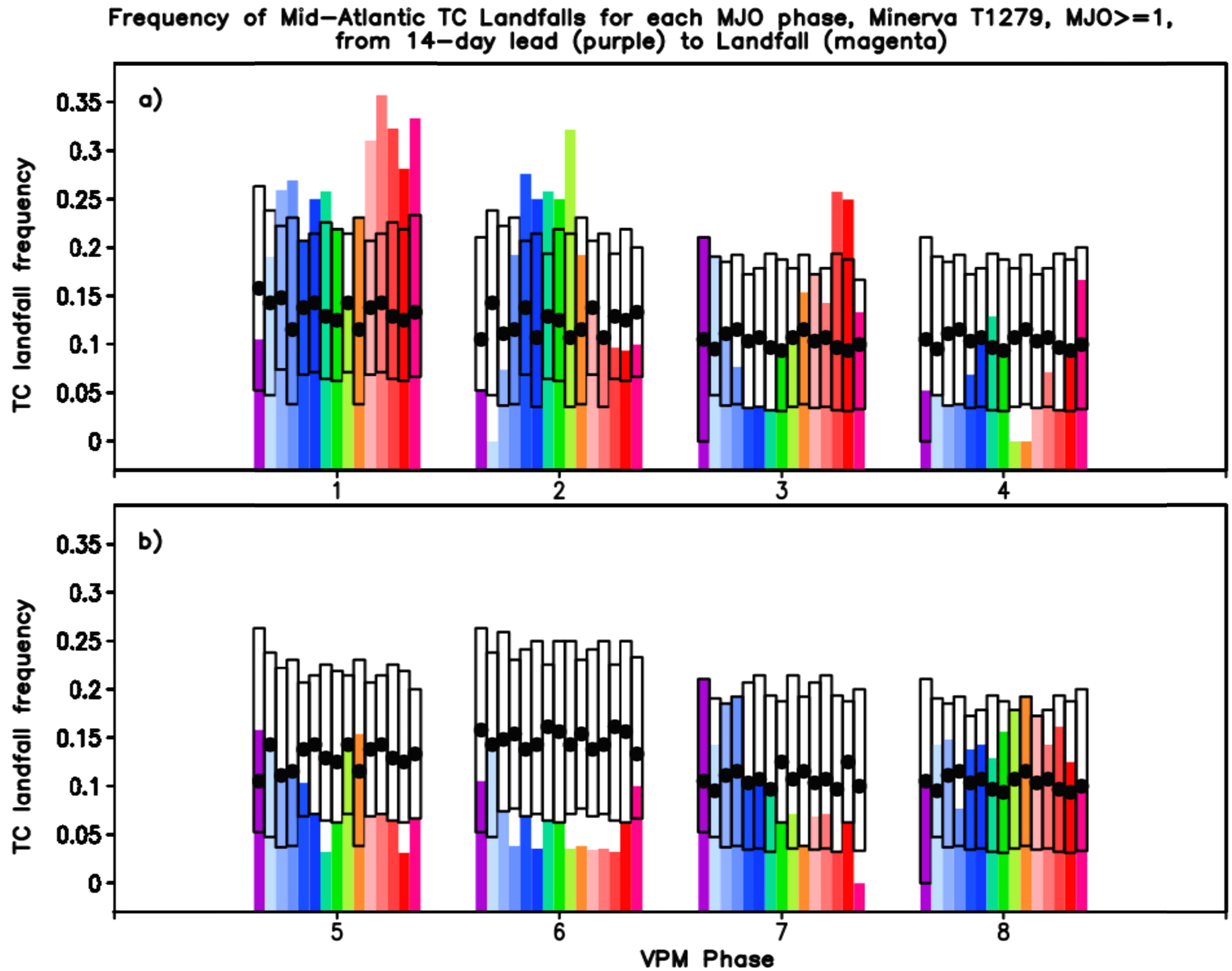

Figure 3: Minerva T1279 mid-Atlantic TC landfall frequency (color bars) for each MJO phase represented by model VPM PCs at different lead times ranging from 14 days (purple bar) to landfall (magenta bar). Box plots in black delineate the 10^{th} and 90^{th} percentiles; dots represent the median. See text for more detail.

4 Discussion and Conclusions

This study uses ensemble seasonal hindcasts with a high-atmospheric-resolution coupled prediction system based on the ECMWF System 4 (Project Minerva) to investigate the MJO modulation of mid-Atlantic TC landfalls, which are among the most infrequent landfalls along the U.S. East Coast. Minerva retrospective forecasts at the highest atmospheric horizontal spectral resolution of T1279 (16-km grid spacing) have been previously shown to achieve reasonable skill in predicting basinwide and regional seasonal TC activity (Manganello et al., 2016). It has been demonstrated that these forecasts are also skillful in reproducing basic statistics and climatological characteristics of mid-Atlantic TC landfalls, which in addition have been found to be predictable on synoptic time scales (Manganello et al., 2019).

Using the VPM index of Ventrice et al. (2013) to diagnose the daily phase and amplitude of the MJO, we find that mid-Atlantic TC landfalls occur more frequently during certain VPM phases compared to others. VPM phases 1-3 are the most favorable phases for these TC landfalls to occur, as they are associated with statistically significant peak landfall frequencies. Our results also suggest that in the extended range, phases 1 and 2 are strongly favored. Whereas in the short range, it is mostly phase 1 and also 3. These results are consistent with a number of previous studies. Klotzbach (2010) has found that the highest levels of the Atlantic TC activity, including the U.S. landfalls, take place during RMM phases 1 and 2 in association with reduced VWS, anomalously high moisture and enhanced low-level cyclonic relative vorticity. In the work of Ventrice et al. (2011), RMM phases 1-3 are the most favorable for the tropical cyclogenesis in the main development region (MDR; 5°-25°N, 60°-15°W) due to similar large-scale environmental changes and enhanced AEW activity over tropical Africa. The latter results have been largely confirmed by Ventrice et al. (2013) using the VPM index. Similarly, Minerva hindcasts show reduced VWS over the western tropical North Atlantic and off the coast of West Africa during the VPM phase 1, and in the MDR and eastern Caribbean during phases 2 and 3 (see Fig. S3). Reduced lower-tropospheric geopotential height and westerly wind anomalies implying enhanced cyclonic vorticity are also present over tropical North Atlantic and western Africa during phases 2 and 3 (see Fig. S4). These changes would favor the formation and development of the land-falling TCs, particularly the ones that originate in the eastern tropical Atlantic. An indication of enhanced convection over the Indian Ocean during VPM phases 2 and 3 (Figs. 2 and S4), albeit more to the west compared to observations, is also consistent with the analysis of Hurricane Sandy's westward steering flow by Ding et al. (2019). While all these factors point in the right direction, additional work is needed to better understand the intraseasonal forcings and mechanisms responsible for these land-falling events. That is, how remote extratropical teleconnections that modulate the steering flow as suggested by Ding et al. (2019), tropical pathways like AEWs and equatorial Rossby waves (see Ventrice et al., 2011) and local influences by means of large-scale environmental changes, within the envelope of the MJO, impact the genesis, development and tracks of TCs that eventually make landfall over the U.S. mid-Atlantic region.

The clear implication of this study is the potential for extended-range forecasts of the mid-Atlantic TC landfall risk based on the phase of the MJO. State-of-the-art ensemble prediction systems display significant skill in the MJO forecasting beyond two weeks (e.g., Vitart, 2017). This progress along with recent improvements in the dynamical predictions of the TC genesis risk in the same time range would make such undertaking feasible.

Acknowledgments

Funding of COLA for this study is provided by grants from NSF (AGS-1338427), NOAA (NA14OAR4310160), and NASA (NNX14AM19G). Special thanks to the European Centre for Medium-Range Weather Forecasts, particularly Franco Molteni and Frederic Vitart, for designing, planning, and conducting some of the simulations as part of the Minerva project. The model output used to generate the plots is publicly available at the COLA data portal ftp://cola.gmu.edu/pub/. A publicly available version of the ECMWF code can be found at https://confluence.ecmwf.int//display/OIFS/OpenIFS+Home. Computing resources on the Yellowstone supercomputer provided by the National Center for Atmospheric Research and the NCAR Command Language scripts available at https://www.ncl.ucar.edu are also gratefully acknowledged.

References

Barrett, B. S., & Leslie, L. M. (2009), Links between tropical cyclone activity and Madden-Julian Oscillation phase in the North Atlantic and Northeast Pacific basins. Monthly Weather Review, 137, 727-744. doi:10.1175/2008MWR2602.1

Blake, E. S., Kimberlain, T. B., Berg, R. G., Cangialosi, J. P., & Beven II, J. L. (2013), Tropical Cyclone Report, Hurricane Sandy (22–29 October 2012). NHC Tech. Rep. AL182012, National Hurricane Center, 157 pp., https://www.nhc.noaa.gov/data/tcr/AL182012_Sandy.pdf.

Dailey, P. S., Zuba, G., Ljung, G., Dima, I. M., & Guin, J. (2009), On the relationship between the North Atlantic sea surface temperatures and U.S. hurricane landfall risk. *Journal of Applied Meteorology and Climatology*, 48, 111-129. doi:10.1175/2008JAMC1871.1

Dee, D. P., and Coauthors (2011), The ERA-Interim reanalysis: Configuration and performance of the data assimilation system. *Quarterly Journal Royal Meteorological Society*, 137, 553–597. doi:10.1002/qj.828

Ding, L., Li, T., Xiang, B., & Peng, M. (2019), On the westward turning of Hurricane Sandy (2012): effect of atmospheric intraseasonal oscillations. *Journal of Climate*, 32, 6859-6873. doi:10.1175/JCLI-D-18-0663.1

European Centre for Medium-Range Weather Forecasts (2013), IFS documentation—CY38r1. ECMWF, accessed 12 September 2018, https://www.ecmwf.int/en/forecasts/documentation-and-support/changes-ecmwf-model/ifs-documentation.

Gottschalck, J., Wheeler, M., Weickmann, K., Vitart, F., Savage, N., Lin, H., Hendon, H., Waliser, D., Sperber, K., Prestrelo, C., Nakagawa, M., Flatau, M., & Higgins, W. (2010), A framework for assessing operational model MJO forecasts: A project of the CLIVAR Madden – Julian Oscillation Working Group. *Bulletin of the American Meteorological Society*, 91, 1247–1258. doi:10.1175/2010BAMS 2816.1

Hodges, K. I. (1994), A general method for tracking analysis and its application to meteorological data. *Monthly Weather Review*, 122, 2573–2586. doi:10.1175/1520-0493(1994)122<2573:AGMFTA>2.0.CO;2

Hodges, K. I. (1995), Feature tracking on the unit sphere. *Monthly Weather Review*, 123, 3458–3465. doi:10.1175/1520-0493(1995)123<3458:FTOTUS>2.0.CO;2

Hodges, K. I. (1999), Adaptive constraints for feature tracking. *Monthly Weather Review*, 127, 1362–1373. doi:10.1175/1520-0493(1999)127<1362:ACFFT>2.0.CO;2

Huang, C. S. Y., & Nakamura, N. (2016), Local finite-amplitude wave activity as a diagnostic of anomalous weather events. *Journal of Atmospheric Sciences*, 73, 211–229. doi:10.1175/JAS-D-15-0194.1

Klotzbach, P. J. (2010), On the Madden-Julian Oscillation – Atlantic hurricane relationship. *Journal of Climate*, 23, 282-293. doi:10.1175/2009JCLI2978.1

Klotzbach, P. J., & Oliver, E. C. (2015), Modulation of Atlantic basin tropical cyclone activity by the Madden-Julian Oscillation (MJO) from 1905 to 2011. *Journal of Climate*, 28, 204-217. doi:10.1175/JCLI-D-14-00509.1

Li, T. (2014), Recent advance in understanding the dynamics of the Madden-Julian oscillation. *Journal of Meteorological Research*, 28(1), 001–033. doi:10.1007/s13351-014-3087-6

Madden, R. A., & Julian, P. R. (1994), Observations of the 40-50-day tropical oscillation – a review. *Monthly Weather Review*, 122, 814-837.

Madec, G. (2008), NEMO ocean engine. Note du Pole de modélisation, Institut Pierre-Simon Laplace (IPSL), Tech.Rep. 27, 396 pp., https://www.nemo-ocean.eu/wp-content/uploads/NEMO_book.pdf.

Manganello, J. V., and Coauthors (2016), Seasonal forecasts of tropical cyclone activity in a high-atmospheric-resolution coupled prediction system. *Journal of Climate*, 29, 1179–1200. doi:10.1175/JCLI-D-15-0531.1

Manganello, J. V., Cash, B. A., Swenson, E. T., & Kinter III, J. L. (2019), Assessment of climatology and predictability of mid-Atlantic tropical cyclone landfalls in a high-atmospheric-resolution seasonal prediction system. *Monthly Weather Review*, 147, 2901-2917. doi:10.1175/MWR-D-19-0107.1

Mo, K. C. (2000), The association between intraseasonal oscillations and tropical storms in the Atlantic basin. *Monthly Weather Review*, 128, 4097-4107.

NHC (2018), Costliest U.S. tropical cyclones tables updated. National Hurricane Center, accessed 29 May 2018, 3 pp., https://www.nhc.noaa.gov/news/UpdatedCostliest.pdf.

Shen, B.-W., DeMaria, M., Li, J.-L. F., & Cheung, S. (2013), Genesis of Hurricane Sandy (2012) simulated with a global mesoscale model. *Geophysical Research Letters*, 40, 4944-4950. doi:10.1002/grl.50934

Ventrice, M. J., Thorncroft, C. D., & Roundy, P. E. (2011), The Madden-Julian Oscillation's influence on African easterly waves and downstream tropical cyclogenesis. *Monthly Weather Review*, 139, 2704-2722. doi:10.1175/MWR-D-10-05028.1

Ventrice, M. J., Wheeler, M. C., Hendon, H. H., Schreck III, C. J., Thorncroft, C. D., & Kiladis, G. N. (2013), A modified multivariate Madden-Julian Oscillation index using velocity potential. *Monthly Weather Review*, 141, 4197-4210. doi:10.1175/MWR-D-12-00327.1

Vitart, F. (2009), Impact of the Madden Julian Oscillation on tropical storms and risk of landfall in the ECMWF forecast system. *Geophysical Research Letters*, 36, L15802. doi:10.1029/2009GL039089

Vitart, F. (2017), Madden-Julian Oscillation prediction and teleconnections in the S2S database. *Quarterly Journal Royal Meteorological Society*, 143, 2210-2220. doi:10.1002/qj.3079

Wheeler, M. C., & Hendon, H. H. (2004), An all-season real-time multivariate MJO index: Development of an index for monitoring and prediction. *Monthly Weather Review*, 132, 1917–1932.

Xiang, B., & Coauthors (2015), Beyond weather time-scale prediction for Hurricane Sandy and Super Typhoon Haiyan in a Global Climate Model. *Monthly Weather Review*, 143, 524–535. doi:10.1175/MWR-D-14-00227.1